PHILOSOPHICAL TRANSACTIONS OF THE ROYAL SOCIETY A MATHEMATICAL, PHYSICAL & ENGINEERING SCIENCES

Lateral Quantum Size Effects Created by Growth Induced Surface and Interface Corrugations on Non-(100)-Oriented Substrates

Klaus H. Ploog and Richard Notzel

Phil. Trans. R. Soc. Lond. A 1993 **344**, 469-480
doi: 10.1098/rsta.1993.0101

Lateral quantum size effects created by growth induced surface and interface corrugations on non-(100)-oriented substrates

By Klaus H. Ploog[1] and Richard Nötzel[2]

[1] *Paul-Drude-Institut für Festkörperelektronik, D-10117 Berlin, F.R.G.*
[2] *Max-Planck-Institut für Festkörperforschung, D-70569 Stuttgart, F.R.G.*

The evolution of periodic arrays of macrosteps and facets on III–V semiconductor surfaces during molecular beam epitaxy is used to create lateral quantum size effects in GaAs quantum wire and quantum dot structures in an AlAs matrix. We show that well ordered alternating wide and narrow regions of GaAs and AlAs form symmetric and asymmetric quantum-dot arrays on (111) and (211) GaAs, respectively, and periodic quantum wire arrays on (311) GaAs. The accumulation of steps by step bunching on (210) GaAs allows us to fabricate mesoscopic step arrays in GaAs–AlAs multilayer structures with a lateral periodicity comparable to the exciton Bohr radius. The observed optical properties of these corrugated multilayer structures confirm the additional lateral size quantization.

1. Introduction

The quantum confinement of electrons and holes in artificial low-dimensional semiconductor structures strongly modifies their electronic properties which has an important impact on the performance of high-speed electronic and photonic devices (Weisbuch 1993). The condition for the occurrence of new electronic phenomena in such structures is that the size of the active region being smaller than the coherence and elastic scattering lengths of the carriers. Advanced crystal growth techniques, such as molecular beam epitaxy (MBE) and metalorganic vapour phase epitaxy (MOVPE), are now routinely used to fabricate artificially layered semiconductors of high structural perfection (Ploog 1988) which exhibit a quasi-two-dimensional (2D) quantization of free carriers. Additional lateral quantum-size effects occur in quantum wire (QWR) and quantum dot (QD) structures having structural features reduced to below 500 Å in size, i.e. to the range of the de Broglie wavelength.

As yet the fabrication of QWR and QD structures has mainly been tried by means of subsequent lateral patterning of 2D heterostructures with nanoscale lithographic techniques (Reed *et al.* 1988; Kash *et al.* 1991; Kohl *et al.* 1989). The minimum lateral dimensions achieved in such structures are much larger than the vertical ones given by epitaxy, hence leading to relatively small separations of the subband energies. These narrow subband spacings are then often masked by the level broadening due to irregularities and defects introduced during the patterning process. To reduce especially the defect density, several methods for direct fabrication of QWR and QD structures based on epitaxial growth have been exploited. In these structures, lateral dimensions comparable to the vertical ones can be achieved. Hence, they allow in

Phil. Trans. R. Soc. Lond. A (1993) **344**, 469–480
Printed in Great Britain

principle for the large subband separations required for optical and electrical device applications (Sakaki 1990). The cleaved-edge overgrowth which forms one-dimensional (1D) structures by growth on the cleaved edge of a 2D heterostructure (Gershoni 1990), the overgrowth of prepatterned V-grooved substrates (Kapon *et al.* 1989; Shen *et al.* 1993), and the generation of supersteps (Sato *et al.* 1990; Yamamoto *et al.* 1993) have been investigated. The formation of lateral superlattices by growth on vicinal substrates has become most prominent. Here, the lateral potential is provided by depositing fractions of a monolayer of material with higher (AlAs) (Sundaram *et al.* 1991) or lower (InAs) (Brandt *et al.* 1991) bandgap compared to GaAs which accumulates at the step edges on vicinal GaAs substrates inclined by a small misorientation to singular surfaces. Due to the height of these steps of only one monolayer, however, efficient lateral confinement requires the creation of lateral columns of material with alternating composition by subsequent deposition of regular fractional monolayers. This imposes tremendous demands on the stability of the growth rates and step uniformity which is hardly achievable due to a poor control of the local misorientation and the kink formation.

In this paper we describe a new concept to directly synthesize GaAs QWR and QD structures in an AlAs matrix by conventional elemental-source MBE. The concept is based on the evolution of well-ordered surface and interface structures on non-(100)-oriented GaAs during epitaxy. Under typical MBE growth conditions, these nominally flat surfaces with high surface energy break up into regular arrays of macrosteps (facets) with spacings and heights of nanometer dimensions to lower the surface energy (Nötzel *et al.* 1991). Self-organization during growth leads to a conservation of the surface corrugation during homoepitaxy and to a unique phase change during heteroepitaxy of AlAs on GaAs and vice versa. The resulting GaAs–AlAs multilayer structures then contain periodically alternating wide and narrow regions of GaAs and AlAs which form symmetric and asymmetric QD structures on (111) and (211) substrates and QWR structures on (311) substrates. Finally, the accumulation of steps by step bunching on (210) GaAs makes feasible the fabrication of mesoscopic step arrays in GaAs–AlAs multilayer structures having a periodicity which is comparable to the exciton Bohr radius (Nötzel *et al.* 1993). The existence of lateral quantum-size effects in these new QWR and QD structures is confirmed when reflection high-energy electron diffraction (RHEED), atomic force microscopy (AFM), high resolution electron microscopy (HREM), and by the distinct electronic properties.

2. Fabrication and structural properties

After the standard process of oxide removal from the GaAs substrate at 580–590 °C in the MBE growth chamber (Ploog 1988) the originally flat (111), (211), (311), and (210) surfaces break up into ordered arrays of macrosteps. This distinct faceting which can be monitored directly by RHEED is preserved during epitaxial growth under standard conditions, i.e. growth rate 0.3–1.2 μm h^{-1}, group-V-to-III flux ratio 5:1, and substrate temperature 580–600 °C. To facilitate the discussion, we briefly specify the reciprocal space of ordered surface structures, which is directly imaged by the RHEED patterns (Henzler 1982; Lagally *et al.* 1988). The asymmetric step array of upward or downward steps is presented in figure 1*a*. The lateral periodicity I and the step height h are deduced from the horizontal splitting of the streaks into slashes and from the length of the streaks normal to the surface, respectively. The lattice constant a of the terrace plane is determined from the

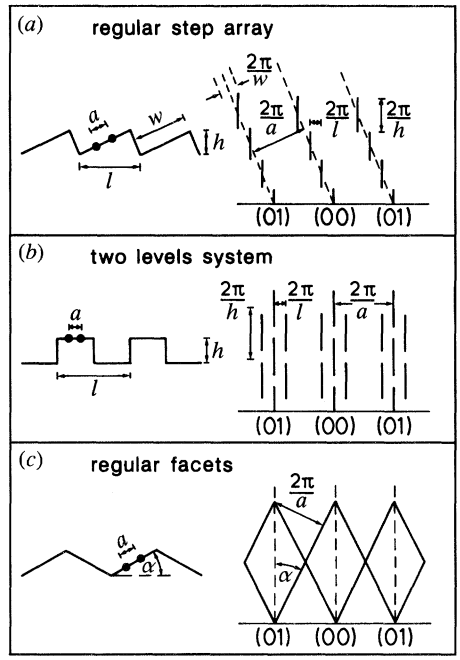

Figure 1. Periodic surface structures with their representation in reciprocal space (*a*) regular step array, (*b*) two-level system, and (*c*) regular facets.

separation of the corresponding streaks which are oriented along the lines connecting the intensity maxima of the slashes (dashed lines). The terrace width w is estimated from the full-width at half-maximum of the streaks corresponding to the terrace planes. The reciprocal space of a two-level system with symmetrically arranged upward and downward steps (figure 1*b*) exhibits streaks which are split alternatingly into satellites and along their length. Intensity maxima of the satellites correspond to intensity minima of the integral order streaks and vice versa. The lateral periodicity l and step height h are deduced from the separation of the satellites and the splitting along the streaks, respectively. The reciprocal space of regular facets exhibits a periodic arrangement of tilted streaks (figure 1*c*). The tilt angle of the facet plane with respect to the nominal surface is determined from the tilt angle of the streaks to the surface normal. The lattice constant a of the facet plane is determined from the streak separation.

The RHEED pattern of the (211) surface shows reversible facetting of the flat surface at temperatures above 590 °C (the transition occurs continuously in the range 550–590 °C). Observation along the [01$\bar{1}$] azimuth above 590 °C (figure 2*a*) exhibits a stepped surface with the step edges along [00$\bar{1}$]. The lateral periodicity l and step height h of the regular step array amount to $l = 9.8$ Å ($= 2a_{111}$) and $h = 2.3$ Å. The terrace width w is estimated to $w = 9.6$ Å. The (111) surface configuration in [01$\bar{1}$] projection of the terrace plane follows from the lattice constant $a = 3.4$ Å ($= a_{211}$). Below 550 °C the RHEED pattern taken along [01$\bar{1}$] becomes diffuse showing a high degree of disorder of the flat (211) surface which is also revealed by the broad 00 streak for the perpendicular [$\bar{1}$11] azimuth. Above 590 ° the RHEED pattern taken along [$\bar{1}$11] (figure 2*b*) shows again slashes tilted by 30 °C to the surface normal, indicating the presence of {110} facets. The extension of these slashes is comparable to those observed along [01$\bar{1}$] (figure 2*a*) thus evidencing the commensurability of the

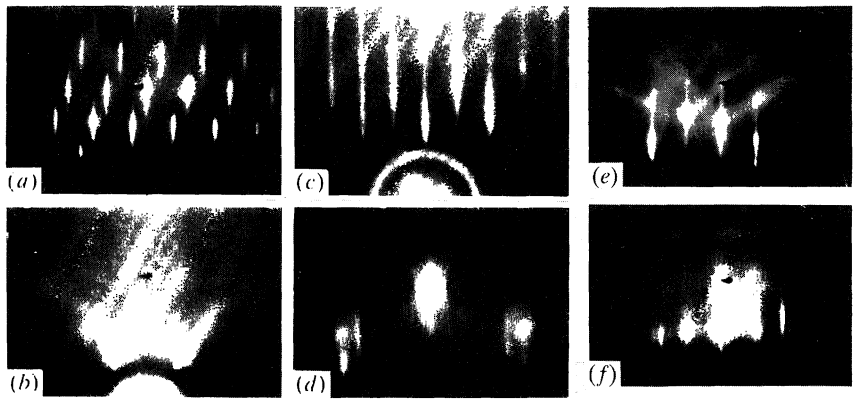

Figure 2. RHEED patterns taken at 30 keV of the (211) GaAs surface (*a*) along [01$\bar{1}$], (*b*) along [$\bar{1}$11], of the (311) GaAs surface (*c*) along [01$\bar{1}$], (*d*) along [$\bar{2}$33], and of the (111) GaAs surface (*e*) along [1$\bar{1}$0], and (*f*) along [11$\bar{2}$].

steps and facets. As a consequence, the stepped (211) surface comprises two sets of {110} facets along [$\bar{1}$11] and alternating (111) terrace planes of 6.9 Å width ($= 2a_{211}$) and (001) steps of 4 Å width ($= a_{100}$) along [01$\bar{1}$] forming asymmetric pyramids of 2.3 Å height ($= 2d_{211}$).

The RHEED pattern of the (311) surface taken along [01$\bar{1}$] reveals a pronounced streaking (figure 2*c*) which indicates a high density of steps along the perpendicular [$\bar{2}$33] direction. Taking the [$\bar{2}$33] azimuth parallel to the steps (figure 2*d*) the RHEED pattern directly images the reciprocal lattice of an almost perfect two-level system oriented along [$\bar{2}$33]. Contrary to the case of the (211) surface, the RHEED pattern of the stepped (311) surface is stable down to room temperature. The lateral periodicity l and step height h amount to $l = 32$ Å ($= 8a_{110}$) and $h = 10$ Å. The extinction of the main streak intensity for maximum intensity of the satellites evidences the high degree of ordering. These experimental parameters agree perfectly with our model describing the surface to be composed of (311) terraces of 4 Å width ($= a_{110}$) and two sets of (33$\bar{1}$) and ($\bar{3}$1$\bar{3}$) facets corresponding to upward and downward steps of 10.2 height ($= 6d_{311}$) having a low surface energy (see figure 4*a*) (Chadi 1984).

The RHEED pattern of the (111) surface shows a pronounced splitting along the integral order streaks which is observed along arbitrary azimuthal directions (figure 2*e*, *f* for the [1$\bar{1}$0] and [11$\bar{2}$] directions). Hence, this splitting reflects the height of the surface structure of the (111) plane amounting to 13 Å. Splitting across the streaks is not resolved, indicating the lateral periodicity exceeding the transfer width of our RHEED system of about 100 Å. From the high symmetry of the [111] crystallographic direction this surface is assumed to break up into symmetric pyramids of 13 Å height ($= 4d_{111}$).

As the surface and interface ordering on (311) GaAs is at present best understood (Nötzel *et al.* 1992*a*, *b*), we will discuss this orientation in some detail. During growth of (311) GaAs/AlAs multilayer structures the RHEED intensity dynamics shows a pronounced oscillation at the onset of GaAs and AlAs growth, respectively (figure 3). This oscillation corresponds to the deposition of three (311) monolayers (ML), i.e. lattice planes, as deduced from the growth rates. During deposition of the next three ML the intensity approaches the value found in the RHEED pattern of the stable stepped surface during growth. The whole sequence then comprises the deposition of six (311) lattice planes, i.e. 10.2 Å, as shown in the inset of figure 3 for different

PHILOSOPHICAL TRANSACTIONS OF THE ROYAL SOCIETY A MATHEMATICAL, PHYSICAL & ENGINEERING SCIENCES

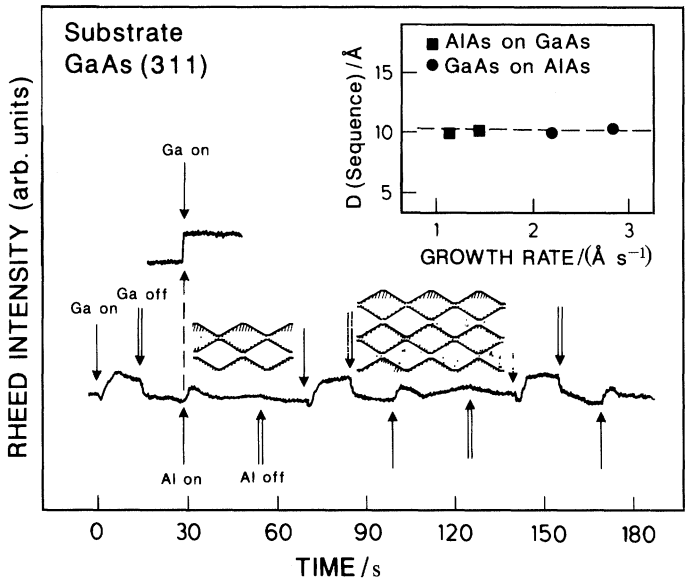

Figure 3. RHEED intensity dynamics taken along [$\bar{2}33$] during growth of (311) GaAs–AlAs multilayer structures. The upper curve shows the RHEED intensity during deposition of GaAs on GaAs. The inset shows the deposited layer thickness for different growth rates of GaAs on AlAs and vice versa until stable growth conditions are reached. The schematic drawing images the GaAs–AlAs multilayer structure resulting from the phase change of the surface corrugation during the heterogeneous deposition of the first monolayers of GaAs and AlAs.

growth rates of GaAs and AlAs. This sequence results from a phase change of the surface corrugation during the heterogeneous deposition of GaAs on AlAs and vice versa. The phase change includes quasi-filling of the corrugation during the first three ML deposition and re-arrangement of the stepped surface during the next three ML deposition. After completion of the phase change, the growth continues layer by layer with conservation of the surface corrugation as indicated by the constant RHEED intensity of the stepped surface during homogeneous growth. We assume that this phase change is induced by strain which makes the heterogeneous growth on the facets energetically more favourable. The completed GaAs–AlAs multilayer structure then consists of well ordered alternating thicker and thinner regions of GaAs and AlAs oriented along [$\bar{2}33$] (figure 3). This unique arrangement indeed forms an as-grown GaAs QWR structure in an AlAs matrix (see figure 4). A very similar behaviour of the RHEED intensity is observed for the growth of GaAs–AlAs multilayer structures on (111) and (211) oriented substrates, so that the phase change of the respective surface corrugation is effective also for these orientations.

The existence of GaAs QWR structures in the AlAs matrix is confirmed by HREM, as shown in figure 4*b*, *c*. Because of the unintentional misorientation of the (311) substrates by 1° and the microroughness of the interfaces the contrast between GaAs and AlAs is not too sharp. Nevertheless, detailed X-ray diffraction measurements reveal that the structural perfection of GaAs–AlAs multilayer structures grown on (311), (211), (111), and (210) substrates is as excellent as that of (100) reference samples (Nötzel *et al.* 1992*a*, *b*). In addition, the average GaAs and AlAs layer thickness (neglecting the specific interface corrugation) are found to be comparable to that of the reference sample, i.e. the overall sticking coefficient of Ga an Al is unity for the (311), (211), (111), (210), and (100) orientation.

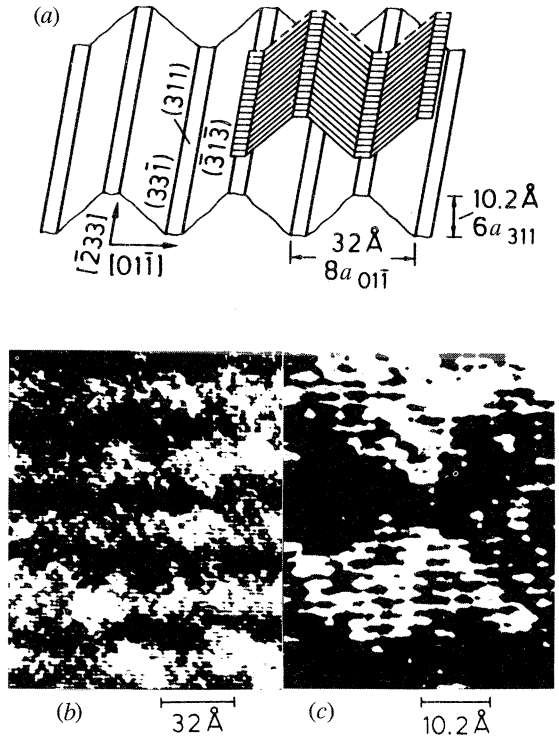

Figure 4. (*a*) Schematic illustration of the stepped GaAs (311) surface. The upper surface (shaded) illustrates the phase change of the surface corrugation during heterogeneous growth of GaAs on AlAs and vice versa. (*b*), (*c*) HREM image of a 15 Å/13 Å (311) GaAs–AlAs multilayer structure viewed along [2̄33].

To increase the periodicity and the step height of the interface corrugations to a range comparable to the exciton Bohr radius (around 100 Å in GaAs), an accumulation of the steps observed on non-(100)-oriented substrates during epitaxy is necessary. The *in situ* formation of 1D mesoscopic surface corrugations on (210) oriented GaAs by step bunching can be directly monitored by RHEED, as depicted in figure 5. The RHEED pattern taken along [001] during growth of GaAs below 560 °C (figure 5*a*) indicates the presence of a regular step array with lateral periodicity of 13 Å, deduced from the horizontal streak separation, and a height of about 3 Å, deduced from the separation of the intensity maxima along the surface normal (Henzler 1982). During GaAs growth above 560 °C, an accumulation of these microscopic steps manifests itself by a continuous transition of the RHEED pattern from figure 5*a* to *b*. The appearance of tilted, non-periodically arranged streaks shows the presence of mesoscopic facets. The tilt angle of the streaks relative to the surface normal gives the tilt angle of the facet planes to about 6° off the singular (100) and (110) planes. During growth of AlAs on the facets at 600 °C, however, the RHEED pattern of figure 5*a* returns, indicating a 'flattening' of the surface. The change towards microscopic steps during growth of AlAs is governed by the lower migration length of Al compared to Ga (Joyce 1990; Hata *et al.* 1990). The high uniformity of the mesoscopic step array and the homogeneous coverage of the surface after GaAs growth above 560 °C is indicated by the high intensity of the tilted streaks in figure 5*b* and by the extinction of 5*a*. The homogeneity is further evidenced by the

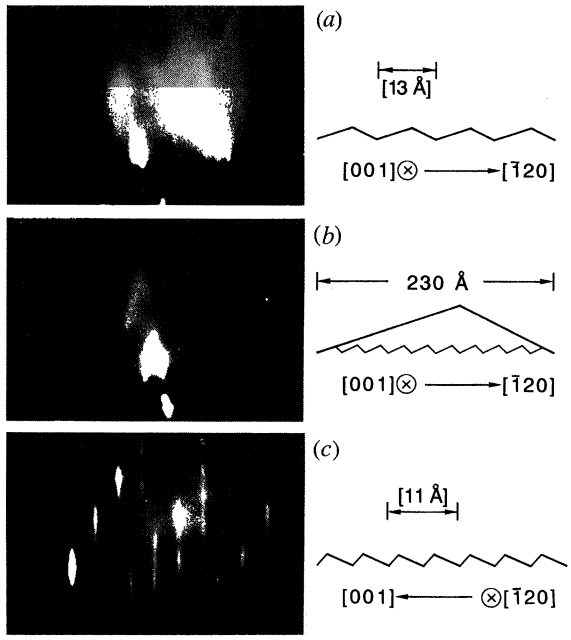

Figure 5. RHEED patterns and schematic illustration of surface corrugations on (210) GaAs taken along [001] during GaAs growth at 500 (*a*), taken along [001] during GaAs growth at 600 °C (*b*), and taken along [$\bar{1}$20] (*c*).

pronounced streaking of the RHEED pattern taken along the perpendicular [$\bar{1}$20] azimuth (figure 5*c*), which is not affected by the step accumulation observed along [001]. This latter RHEED pattern arises from the periodic step array of the microscopic surface configuration of the (210) plane with a lateral periodicity of 5.6 Å and a step height of 2.6 Å.

The actual size of the mesoscopic steps is determined from RHEED intensity dynamics during the growth of GaAs–AlAs multilayer structures at 600 °C (Nötzel *et al.* 1993). The time of step accumulation during growth of GaAs on AlAs and the time of filling the surface corrugation during growth of AlAs on GaAs can be deduced from the time dependence of the RHEED intensity of the streaks originating from the microscopically stepped surface. Together with the corresponding growth rates a height of the steps of about 20 °C is deduced. This value together with the tilt angle of the streaks in figure 5*b* gives a lateral width of the steps of about 200 Å.

The topography of the mesoscopic surface corrugation after GaAs growth at 600 °C can be directly imaged by AFM. In figure 6 we show a AFM topographical image (Nötzel *et al.* 1993). From the single line scan perpendicular to the step array in figure 6*b* the lateral periodicity is determined to be 230 Å. This value is in good agreement with the periodicity deduced from the RHEED dynamics. The actual height of the steps is not imaged accurately by the AFM single line scan (about 10 Å), due to the fast oxidation of the sample after removal from the MBE growth chamber which partly smoothens the surface corrugation and introduces fluctuations in the shape of the step array. However, the AFM photograph directly illustrates the high uniformity and almost perfect periodicity of the mesoscopic step array directly formed on (210) GaAs substrates during MBE growth of GaAs.

Direct evidence for the specific shape of the mesoscopic steps in GaAs–AlAs

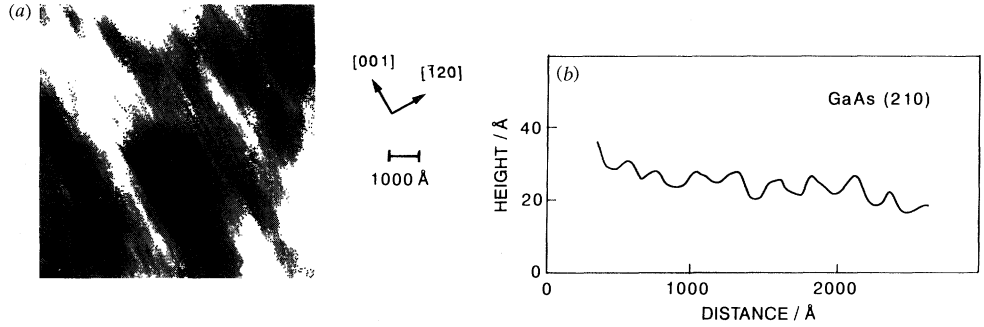

Figure 6. AFM topographical image of (210) GaAs grown at 600 °C (*a*) and single line scan perpendicular to the grooves (*b*) showing the high periodicity of the surface corrugation.

multilayer structures running along [001] comes from HREM imaging (Nötzel *et al.* 1993). The tilt angle of the facets with respect to the macroscopic (210) surface and the step height of 21–23 Å derived from the HREM images are in excellent agreement with the RHEED results.

3. Electronic properties

The photoluminescence (PL) lines of the GaAs QWR and QD structures are always shifted to lower energies as compared to (100) multiple quantum-well (MQW) reference samples grown side by side with the (311), (211), (111), and (210) samples. This red shift arises from the fact that the luminescence originates from the respective wider wire and dot regions. The red shift of the PL obtained from (311), (211), and (111) GaAs–AlAs multilayer structures with the same average GaAs and AlAs thicknesses increases with the height of the surface corrugation in the different orientations (see figure 7 and table 1 for 46 Å GaAs multilayer structures). In addition, we observe an enhancement of the light-hole (LH) exciton continuum energies with the height of the surface corrugation (table 1). The LH exciton continuum energies are deduced from the energy spacing between the LH exciton transition and the supplementary LH transitions observed in the photoluminescence excitation (PLE) spectra (figure 7). Their substantial increase in the (211), (311), and (111) structures directly reflects the additional lateral confinement (Brown & Spector 1987) provided by the specific interface corrugation. The LH character of these transitions is evidenced by the observed negative degree of circular polarization which excludes their origin from 'forbidden' transitions. The increased stability of the confined excitons is also manifested by the strong exciton-phonon interaction which is revealed by the observation of hot-exciton relaxation (Permogorov 1975). When the detection wavelength is set to the high-energy side of the PL line, strong LO and TA phonon related lines are resolved in the PLE spectra of the (311), (211), and (111) samples (figure 7), because of the high probability of the laterally confined excitons created above the bandgap to relax as a whole.

The PLE spectra of the (211) and (311) samples (figure 7*b*, *c*) exhibit a pronounced polarization anisotropy of the excitonic resonances. The LH resonance is more pronounced in the spectrum taken with the light polarized parallel to the [011] direction, whereas the heavy hole (HH) resonance is more pronounced for the respective perpendicular polarization in agreement with the asymmetric interface corrugation in these structures (Citrin & Chang 1991). The corresponding polarization

PHILOSOPHICAL TRANSACTIONS OF THE ROYAL SOCIETY A MATHEMATICAL, PHYSICAL & ENGINEERING SCIENCES

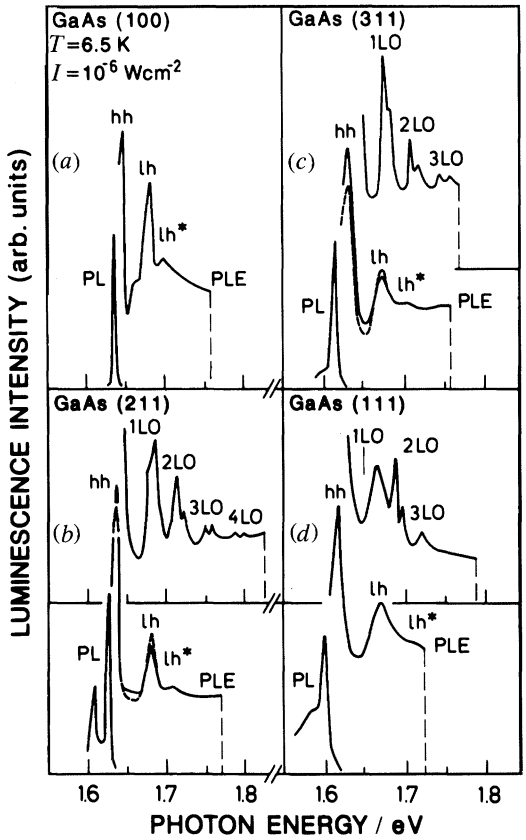

Figure 7. Low-temperature PL and PLE spectra of (*a*) (100), (*b*) 211, (*c*) (311), and (*d*) (111) 46 Å/41 Å GaAs–AlAs multilayer structures. In (*b*) and (*c*) the dashed lines show the PLE spectra for light polarized parallel to the [01$\bar{1}$] azimuth (parallel to the direction of lateral quantization) and the solid lines correspond to the respective perpendicular directions. The sharp LO- and TA-phonon related lines are resolved when the detection energy is set to the high energy side of the PL line.

Table 1. *Dependence of the luminescence redshift and light-hole* (LH) *exciton continuum energy on the surface corrugation height for various orientations*

orientation	(100)	(211)	(311)	(111)
height of surface corrugation/Å	0	2.3	10.2	13.1
red-shift of luminescence/meV	0	16	24	38
LH exciton continuum energy/meV	15	27	29	36

behaviour is observed also in PL. No optical anisotropy is observed for (100) and (111) samples as expected for quantum wells and also for the symmetric surface structure found for the (111) orientation. The additional lateral confinement existing in the (111) sample manifests itself in the strongly increased exciton continuum energy and in the appearance of phonon related lines in the PLE spectra. The LH exciton continuum energy is observed also in the absorption spectrum taken from (111) samples.

It is important to note that the GaAs QWR and QD structures exhibit an extremely high luminescence intensity. In figure 8 we show that at 300 K the integrated PL

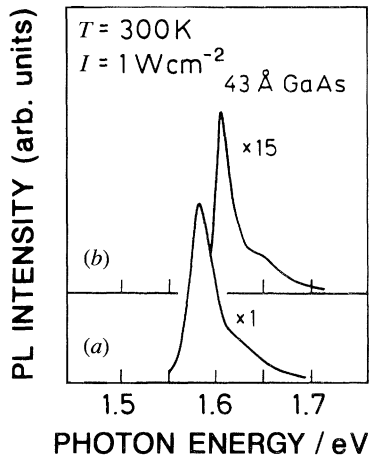

Figure 8. Room-temperature PL of (*a*) a 43 Å/47 Å GaAs–AlAs (311) quantum-wire structure and (*b*) a 43 Å/47 Å GaAs–AlAs (100) multiple quantum-well structure, indicating the red shift and high luminescence intensity of the (311) samples.

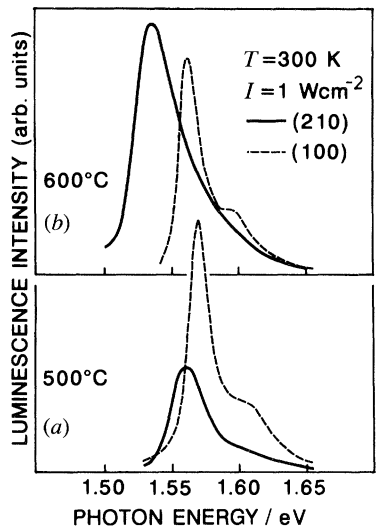

Figure 9. Room-temperature PL of 48 °C GaAs/50 Å AlAs (210) and (100) oriented multilayer structures grown side by side at 500 °C (*a*) and at 600 °C (*b*).

intensity of the (311) QWR structure is by more than one order of magnitude larger than that of the reference (100) MQW sample. This behaviour which does not degrade up to 400 K arises from the additional lateral confinement and strong localization of the excitons in the QWR structures. The non-radiative interface recombination is strongly suppressed due to the reduced spreading of the photogenerated carriers whose motion is now free along the wire direction. This finding is important for the design of light emitting devices of high efficiency.

The unique growth behaviour of GaAs and AlAs on (210) GaAs above and below 560 °C offers a new flexibility in engineering GaAs–AlAs interfaces. It allows the formation of GaAs–AlAs multilayer structures with microscopically stepped interfaces at low growth temperatures (no accumulation of steps) and with alternating microscopically and mesoscopically stepped interfaces at elevated growth

temperatures (no accumulation of steps) and with alternating microscopically and mesoscopically stepped interfaces at elevated growth temperatures (accumulation of steps during GaAs growth). The influence of these different interface structures on the optical properties of GaAs–AlAs multilayer structures is illustrated by the room temperature luminesence of samples grown at 500 °C and at 600 °C (figure 9). The formation of mesoscopic steps during GaAs growth at 600 °C results in a 26 meV red shift of the luminescence with respect to that of the (100) reference sample. This value strongly exceeds the 11 meV red shift for the samples grown at 500 °C which is attributed to the presence of microscopic steps. The most important result, however, is again the integrated luminescence intensity of the (210) samples grown at 600 °C which is strongly enhanced compared to that of the (100) reference structure. This behaviour is assigned to a reduced diffusion of carriers in samples with mesoscopic interface corrugation, which is free only along the steps. This reduces the probability to encounter non-radiative recombination centres.

4. Conclusion

The controlled generation of steps and terraces on non-(100)-oriented GaAs surfaces has been used to directly fabricate GaAs QWR and QD structures by epitaxial growth. The formation of regular arrays of macro-steps with spacings and heights in the nanometer range is directly revealed by RHEED. Asymmetric pyramids are formed on the (211) surface, periodic channels on the (311) surface and symmetric pyramids on the (111) surface. The periodicity and the step height of the surface and interface corrugations can be increased to a range comparable to the exciton Bohr radius through the accumulation of steps during MBE growth. In this way, 1D step arrays with a periodicity of more than 200 Å are obtained by step bunching on (210) GaAs. These periodic surface and interface corrugations give rise to additional lateral size quantization in GaAs–AlAs multilayer structures resulting in unusual electronic properties. The observed shift of the luminescence energy, the increased exciton continuum energy, the enhanced exciton–phonon interaction, the distinct optical anisotropy, and the increased integral luminescence intensity directly reflect the existence of additional lateral confinement effects in these GaAs–AlAs multilayers.

Although the results presented here are quite encouraging, the reproducible fabrication of low-dimensional semiconductors having quasi-1D and quasi-0D electronic properties remains one of the major challenges in spatially resolved materials synthesis and, moreover, in the entire field of microstructure materials science. Methods must be developed which enable the manipulation of materials atom-by-atom in well-defined spatial and geometrical arrangements without causing damage to the crystal surface. The described techniques are only one choice for the fabrication of quantum wires and quantum dots. The search for methods and techniques to manipulate the atoms in a crystal one-by-one (growth, removal, displacement) should be extended also to other solid materials.

This work was sponsored by the Bundesministerium für Forschung und Technologie of the Federal Republic of Germany.

References

Brandt, O., Tapfer, L., Ploog, K., Bierwolf, R., Hohenstein, M., Phillipp, F., Lage, H. & Heberle, A. 1991 *Phys. Rev.* B **44**, 8043.

Brown, J. W. & Spector, H. N. 1987 *Phys. Rev.* B **35**, 3009.

PHILOSOPHICAL TRANSACTIONS OF THE ROYAL SOCIETY A MATHEMATICAL, PHYSICAL & ENGINEERING SCIENCES

Chadi, D. J. 1984 *Phys. Rev.* B **29**, 785.

Citrin, D. S. & Chang, Y. C. 1991 *Phys. Rev.* B **43**, 11703.

Gershoni, D., Weiner, J. S., Chu, S. N. G., Baraff, G. A., Vandenberg, J. M., Pfeiffer, L. N., West, K., Logan, R. A. & Tanbun-Ek, T. 1990 *Phys. Rev. Lett.* **65**, 1631.

Hata, M., Isu, T., Watanabe, A. & Katayama, Y. 1990 *J. Vac. Sci. Technol.* B **8**, 692.

Henzler, M. 1982 *Appl. Surf. Sci.* **12**, 450.

Joyce, B. A. 1990 *J. Cryst. Growth* **99**, 9.

Kapon, E., Hwang, D. & Bhat, R. 1989 *Phys. Rev. Lett.* **63**, 430.

Kash, K., Van der Gaag, B. P., Mahoney, D. D., Gozdz, A. S., Florez, L. T., Harbison, J. P. & Sturge, M. D. 1991 *Phys. Rev. Lett.* **67**, 1326.

Kohl, M., Heitmann, D., Grambow, P. & Ploog, K. 1989 *Phys. Rev. Lett.* **63**, 2124.

Lagally, M. G., Savage, D. E. & Tringides, M. C. 1988 In *Reflection high-energy electron diffraction and reflecting elecron imaging of surfaces* (ed. P. K. Larsen & P. J. Dobson), p. 139. NATO Advanced Study Institutes, Ser. B. New York: Plenum.

Nötzel, R., Ledentsov, N. N., Däweritz, L., Hohenstein, M. & Ploog, K. 1991 *Phys. Rev. Lett.* **67**, 3812.

Nötzel, R., Ledentsov, N. N., Däweritz, L., Ploog, K. & Hohenstein, M. 1992*a* *Phys. Rev.* B **45**, 3507.

Nötzel, R., Däweritz, L. & Ploog, K. 1992*b* *Phys. Rev.* B **46**, 4736.

Nötzel, R., Eissler, D. & Ploog, K. 1993 *J. Cryst. Growth* **127**, 1068.

Permogorov, S. 1975 *Phys. Status Solidi* B **68**, 9.

Ploog, K. 1988 *Angew. Chem. Int. Ed. Engl.* **27**, 593.

Reed, M. A., Randall, J. N., Aggarwal, J. R., Matyi, R. J., Moore, T. M. & Wetsel, A. E. 1988 *Phys. Rev. Lett.* **60**, 535.

Sakaki, H. 1990 In *Localization and confinement of electrons in semiconductors* (ed. F. Kuchar, H. Heinrich & G. Bauer), p. 2. Springer Series in Solid-State Sciences, vol. 97. Heidelberg: Springer Verlag.

Sato, M., Maehashi, K., Asahi, H., Hasegawa, S. & Nakashima, H. 1990 *Superlattices and Microstructures* **7**, 279.

Shen, X. Q., Tanaka, M. & Nishinaga, T. 1993 *J. Cryst. Growth* **127**, 932.

Sundaram, M., Chalmers, S. A., Hopkins, P. F. & Gossard, A. C. 1991 *Science, Wash.* **254**, 1326.

Weisbuch, C. 1993 *J. Cryst. Growth* **127**, 742.

Yamamoto, T., Inai, M., Takebe, T. & Kobayashi, K. 1992 *J. Cryst. Growth* **127**, 865.

PHILOSOPHICAL TRANSACTIONS OF THE ROYAL SOCIETY A MATHEMATICAL, PHYSICAL & ENGINEERING SCIENCES

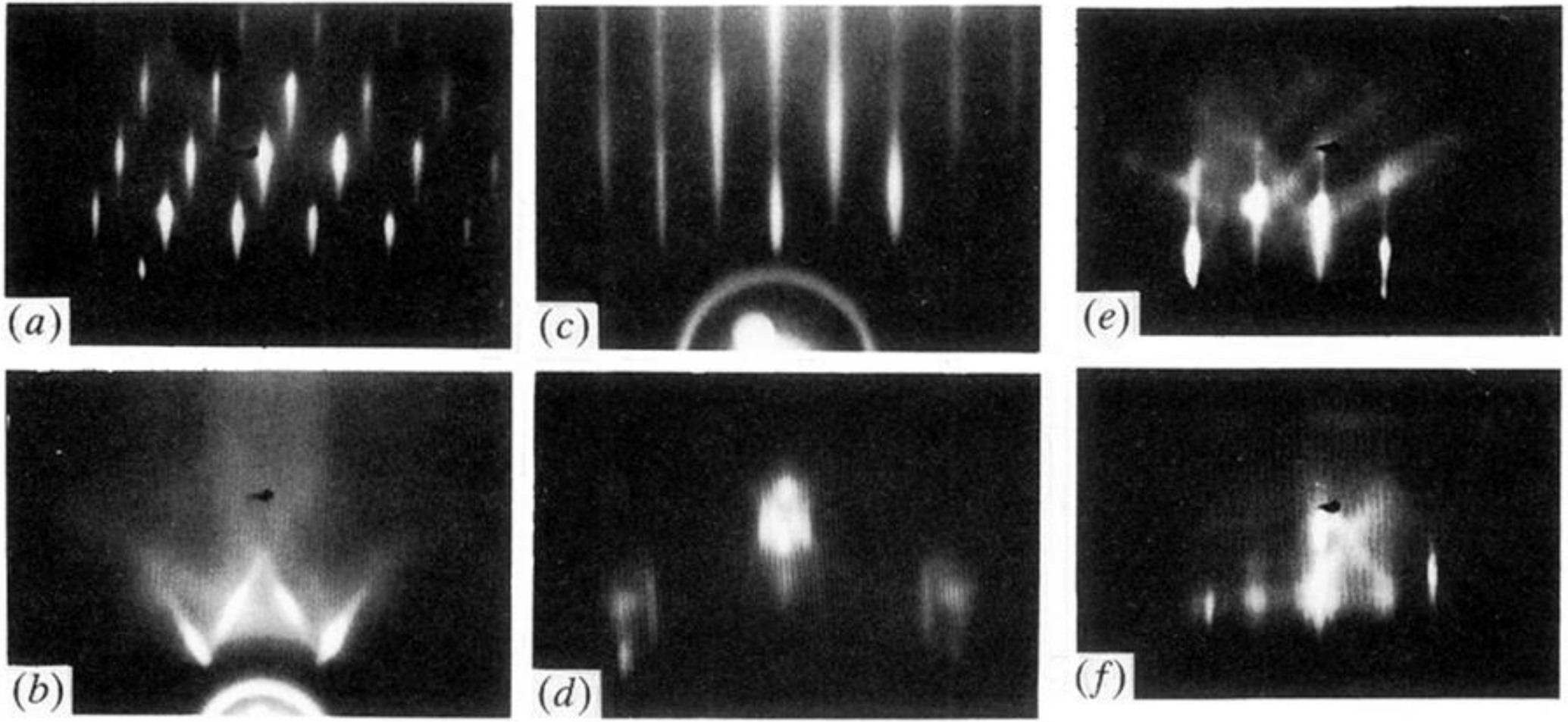

Figure 2. RHEED patterns taken at 30 keV of the (211) GaAs surface (*a*) along [01$\bar{1}$], (*b*) along [$\bar{1}$11], of the (311) GaAs surface (*c*) along [01$\bar{1}$], (*d*) along [$\bar{2}$33], and of the (111) GaAs surface (*e*) along [1$\bar{1}$0], and (*f*) along [11$\bar{2}$].

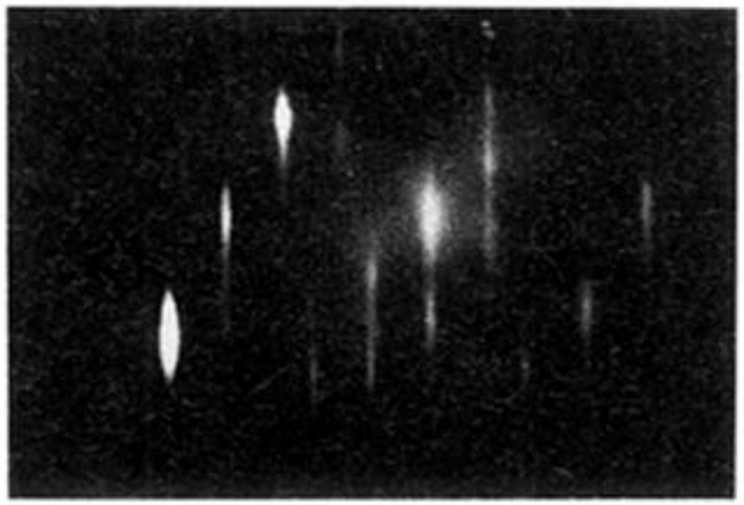

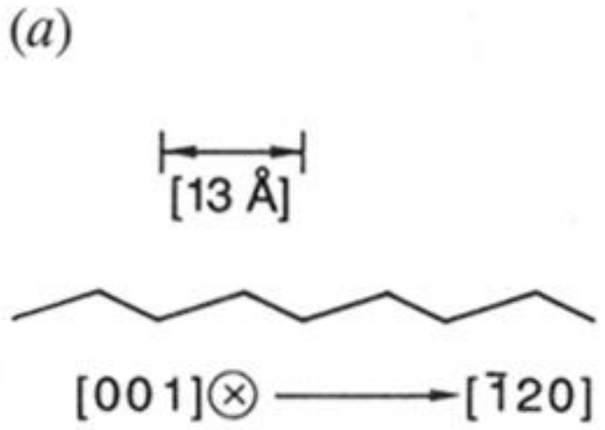

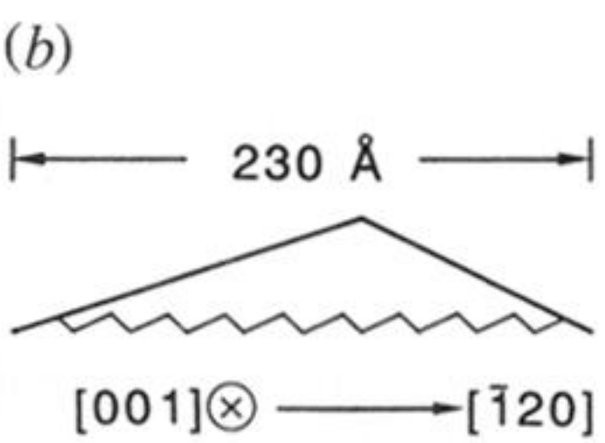

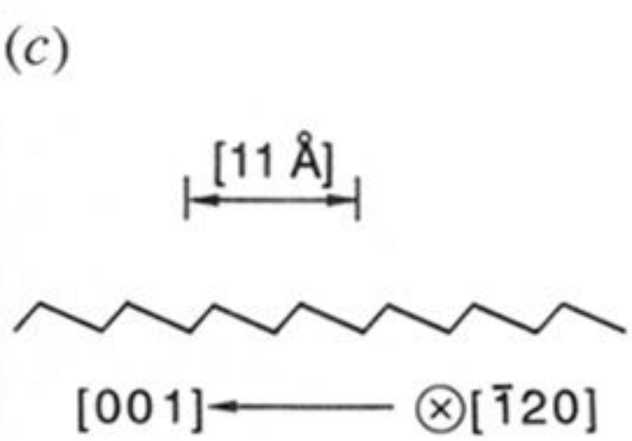

Figure 5. RHEED patterns and schematic illustration of surface corrugations on (210) GaAs taken along [001] during GaAs growth at 500 (*a*), taken along [001] during GaAs growth at 600 °C (*b*), and taken along [$\bar{1}$20] (*c*).

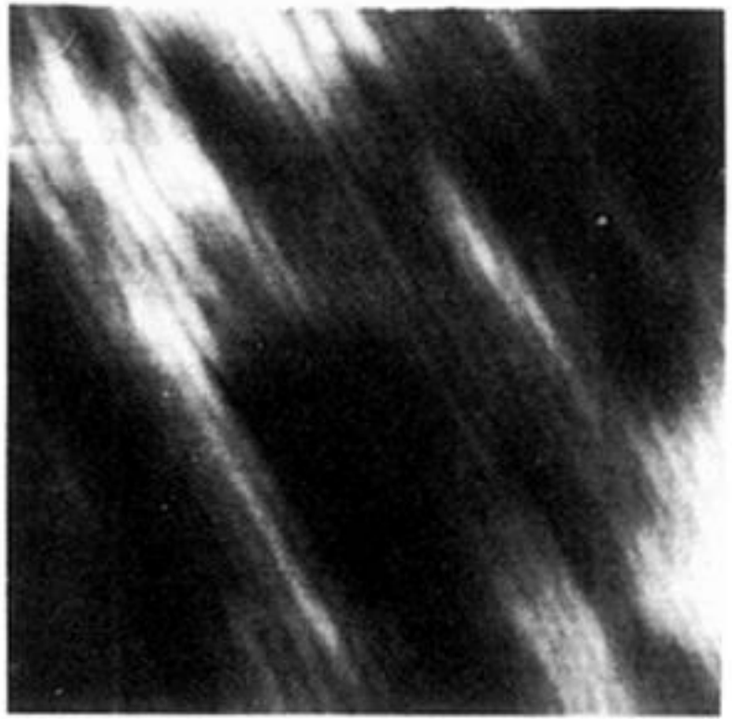

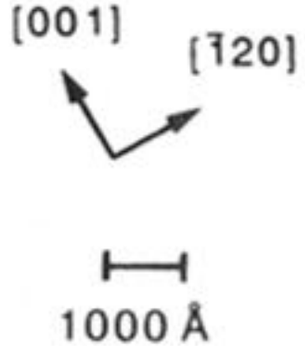

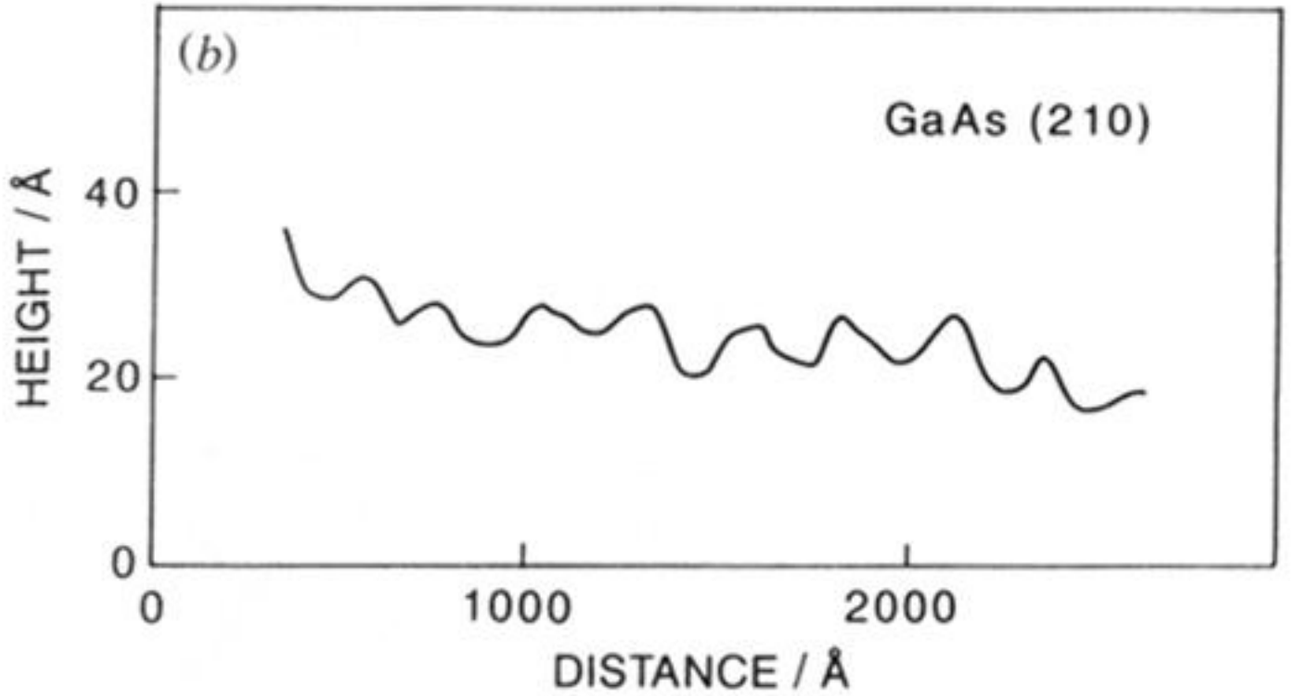

Figure 6. AFM topographical image of (210) GaAs grown at 600 °C (*a*) and single line scan perpendicular to the grooves (*b*) showing the high periodicity of the surface corrugation.